Active Control of Dynamic Supraparticle Structures in Microchannels

Mark A. Hayes,*,† Nolan A. Polson,‡ and Antonio A. Garcia§

Department of Chemistry and Biochemistry and The Center for Solid State Electronics Research, Arizona State University, Tempe, Arizona 85287, ThermoBiostar, Inc., Boulder, CO 80301, and Department of Bioengineering, Arizona State University, Tempe, AZ 85287

Received November 28, 2000. In Final Form: February 7, 2001

Paramagnetic particles in microchannels form dynamic and reversible self-assembled regularly spaced structures when exposed to an external magnetic field. The magnetically induced micron-scale patterns can be formed and reformed spontaneously, thus providing an alternative to traditional microfabrication techniques for pattern creation. Under the influence of a varying magnetic field, these structures could be rotated through all axes without loss of structural form allowing dynamic micron-scale movement without direct mechanical, electrical, or photonic interactions. The structures are not attached to the wall of the enclosure and are free to move without loss of form from both pressure-induced flow and electrokinetic effects. The dynamic supraparticle patterning can be used in an extensive variety of on-chip applications and for unique microfabrication techniques.

Introduction

Microfluidic devices have just begun to find widespread application.[1−6] Based on the foundations of microelectronics and microelectromechanical systems, intensive research has led to extending microdevices to these fluid-based systems.[7−10] Currently, there are numerous innovations that promise to expand the use of such microdevices. Some of these include reliable mixing to aid chemical reactions, simple cellular manipulations for bioanalytical application, integration of microoptical devices such as filters or gratings, and novel, yet simple, fabrication protocols. Generally, each of these innovations has been developed along independent paths, with separate, specific technology. In contrast, a common basis for a variety of innovations is suggested by recent work in our laboratory where paramagnetic particles produce unique, dynamic, and reversible structures in microchannels when the particle−particle interactions are induced and manipulated by an external magnetic field. Lateral movement of the structures can be accomplished using both pressure and electrokinetic flows where no distortion of the supraparticle structures is observed.

The formation of patterns in particle-containing solutions and colloids (ferrofluids and magnetorheological fluids) in macroscale systems has been modeled and observed.[11−15] These studies have shown that an external magnetic field induces the formation of static linear aggregates of paramagnetic particles within colloidal solutions. Periodic structures such as these are often the result of competition among energies, where, in this case, localized magnetic fields, electrostatic interactions, and Brownian motion are competing with the long-range dipole energy. Inducing the formation of these columnar structures can be understood by examining the actions of the individual particles in the presence of an external field. The generation of the pattern is directly related to the ratio of the magnetic interaction energy between the paramagnetic particles (U) relative to the thermal energy (kT) which randomizes the dipoles within the system because of Brownian motion. The magnetic interaction energy of two paramagnetic particles can be described by

$$U(D, \theta) = (m^2/4\pi\mu_0)((1 - 3\cos^2\theta)/D^3) \qquad (1)$$

where m is the induced magnetic dipole, μ_0 is the permeability of free space, θ is the angle between a line connecting the centers and the orienting field, and D is the center-to-center distance of the two particles.[16−18] The

* To whom correspondence should be addressed.
† Department of Chemistry and Biochemistry and The Center for Solid State Electronics Research.
‡ ThermoBiostar, Inc.
§ Department of Bioengineering.

(1) Harrison, D. J.; Fluri, K.; Seiler, K.; Fan, Z.; Effenhauser, C. S.; Manz, A. *Science* **1993**, *261*, 895−897.
(2) Bousse, L.; Cohen, C.; Nikiforov, T.; Chow, A.; Kopf-Sill, A. R.; Dubrow, R.; Parce, J. W. *Annu. Rev. Biophys. Biomol. Struct.* **2000**, *29*, 155−181.
(3) Burns, M. A.; Johnson, B. N.; Brahmasandra, S. N.; Handique, K.; Webster, J. R.; Krishnan, M.; Sammarco, T. S.; Man, P. M.; Jones, D.; Heldsinger, D.; Mastrangelo, C. H.; Burke, D. T. *Science* **1998**, *282*, 484−487.
(4) Kopp, M. U.; de Mello, A. J.; Manz, A. *Science* **1998**, *280*, 1046−1048.
(5) Heller, M. J.; Forster, A. H.; Tu, E. *Electrophoresis* **2000**, *21*, 157−164.
(6) Tokeshi, M.; Minagawa, T.; Kitamori, T. *Anal. Chem.* **2000**, *72*, 1711−1714.
(7) Manz, A.; Harrison, D. J.; Verpoorte, E.; Widmer, H. M. *Adv. Chromatogr.* **1993**, *33*, 1−66.
(8) Seiler, K.; Harrison, D. J.; Manz, A. *Anal. Chem.* **1993**, *65*, 1481−1488.
(9) Harrison, D. J.; Glavina; Manz, A. *Sens. Actuators, B* **1993**, *10*, 107−116.
(10) Manz, A.; Harrison, D. J.; Verpoorte, E. M. J.; Fettinger, J. C.; Paulus, A.; Ludi, H.; Widmer, H. M. *J. Chromatogr.* **1992**, *593*, 253−258.
(11) Wang, H.; Zhu, Y.; Boyd, C.; Luo, W.; Cebers, A.; Rosensweig, R. E. *Phys. Rev. Lett.* **1994**, *72*, 1929−1932.
(12) De Gennes, P. G.; Pincus, P. A. *Phys. Kondens. Mater.* **1970**, *11*, 189−198.
(13) Skjeltorp, A. T. *J. Appl. Phys.* **1985**, *57*, 3285−3290.
(14) Hwang, Y. H.; Wu, X.-L. *Phys. Rev. E* **1994**, *49*, 3102−3108.
(15) Liu, J.; Lawrence, E. M.; Wu, A.; Ivey, M. L.; Flores, G. A.; Javier, K.; Bibette, J.; Richard, J. *Phys. Rev. Lett.* **1995**, *74*, 2828−2831.
(16) Furst, E. M.; Suzuki, C.; Fermigier, M.; Gast, A. P. *Langmuir* **1998**, *14*, 7334−7336.
(17) Sholten, P. C. *J. Magn. Magn. Mater.* **1983**, *39*, 99−106.
(18) Promislow, J. H. E.; Gast, A. P.; Fermigier, M. *J. Chem. Phys.* **1995**, *102*, 5492−5499.

10.1021/la001655g CCC: $20.00
Published on Web 03/28/2001

magnetic dipole is characterized by the following equation:

$$m = (4/3)\pi r_p^3 \chi_p B \quad (2)$$

where r_p is the particle radius, χ_p is the magnetic susceptibility of the material, and B is the magnetic flux density.[16−18] The dimensionless dipole strength λ provides the ratio of the maximum magnetic attraction between two particles to the thermal energy:

$$\lambda = -U_{max}/kT \quad (3)$$

where k is the Boltzmann constant and T is the absolute temperature. When the particle interactions are much stronger than the thermal energy, the particles will align in the direction of the magnetic field. Accordingly, the formation of supraparticle structures is dependent upon the diameter of the particles, the volume fraction of the solution, the magnetic susceptibility, the magnetic field intensity, the channel geometry, the temperature of the system, and the surface properties of the microchannels.

In the presence of an orienting external magnetic field, these equations suggest that growing a one-dimensional lattice by adding particles end-to-end is preferred at low particle concentrations because a larger negative free energy change results.[12,19] However, at higher concentrations a two-dimensional lattice of staggered rows of particles results[17] which is observed as columns in this work and in the work of Wang and colleagues.[11] Similar patterns have been observed by researchers interested in the assembly of polystyrene particles[14] and emulsions[14,15,17] with encapsulated magnetite submicron particles. These researchers and others have presented several mathematical models to explain the end-to-end aggregation of magnetic microspheres in the direction of the magnetic field lines.[13,17,20] Because of lateral attractive forces and size mismatch, these aggregations combine and form columns. Once formed, their poles are aligned and short range ordering is generated because the columns are repulsive to each other. For a given field strength, the characteristic spacing between columns has been described as being strongly influenced by the characteristic width of the container according to a power law relationship.[11,15]

The novel aspect of the supraparticle structures observed within this study is the ability to produce unique structures, in a reversible manner, that can be dynamically manipulated by control of an external magnetic field. No direct physical, optical, or electrical interface is necessary for the physical movements of these supraparticle structures. The preliminary data in this work and the understanding generated by previous paramagnetic systems indicate that by the careful manipulation of systematic properties (particle diameter, particle's inherent magnetic susceptibility, volume fraction, magnetic field intensity, temperature, and channel geometry) the size and spacing of such structures can be directly controlled. The translational motion of these structures through microchannels can be accomplished using electrokinetic or pressure-driven flows without any deformation of the induced form. The ability to dynamically and reversibly form paramagnetic supraparticle structures and control their movement and spacing by external conditions will allow many innovations to be explored for integration onto analytical microdevices.

Materials and Methods

Materials. Sodium dihydrogen phosphate (NaH_2PO_4) was obtained from Aldrich Chemical Co., Inc. (Milwaukee, WI) and was used as received. All NaH_2PO_4 buffers were prepared to a 20 mM concentration and adjusted to pH 7.0 using 1 M sodium hydroxide (Mallinckrodt, Phillipsburg, NJ). Paramagnetic particles (1−2 μm diameters) coated with an amine functional group, containing greater than 20 wt % of iron, and having a polystyrene surface matrix with amine groups were purchased from Polysciences, Inc. (Warrington, PA; catalog no. 18190) and used as received. Dynal paramagnetic particles (2.8 μm diameter, 1 mg/mL diluted 5× in phosphate buffered saline) were a gift from Nichols Institute Diagnostics (San Juan Capistrano, CA). Fused silica capillary (150 μm outer diameter/20 μm inner diameter) was purchased from Polymicro Technologies, Inc. (Phoenix, AZ) and cut to a 50.8 cm length. All buffers and samples were prepared with 18 MΩ purified water drawn from a NANOpure UV ultrapure water filtration system (Barnstead, Dubuque, Iowa).

Apparatus. An in-house-built vacuum/pressure chamber was used to induce pressure differentials across the fused silica capillary. Electroosmotic flows were generated using a capillary electrophoresis system built in-house using a CZE1000R high-voltage power supply (Spellman High Voltage Electronics Corporation, Hauppauge, NY). Pressure flows were generated using a vacuum pump system (CENCO Hyvac, Fort Wayne, IN). An Olympus IX70 Inverted Research microscope (Tokyo, Japan) was used for imaging. Image acquisition in the packed bed areas was performed with an RS170 CCD camera (SCI Electronics, East Hartford, CT) integrated with National Instruments LabVIEW image acquisition software and an IMAQ PCI-1408 image acquisition board (National Instruments, Austin, TX) where imaging programs were developed in-house.

Patterning. The paramagnetic beads were locally packed onto a fused silica capillary by the application of a strong magnetic field (2360 G at the channel wall) by a rare earth magnet (3/4 in. diameter, 0.1875 in. thick disk of NdFeB (27/30 mixed), rated at 11 lb lift (Edmund Scientific, Barrington, NJ; catalog no. CR35-106)). The magnet was placed directly over the microchannel, and the paramagnetic particles were locally collected at the area of the steepest magnetic field gradient (leading edge of the magnet). The particles were flowed through the system using vacuum-induced flows of 0.33 atm for 30 s followed by 0.10 atm for 5−10 min. Fluid flow in the channel can be controlled either by application of a pressure gradient or through electroosmosis. A newly packed bed was used for each experiment. Typical packed bed lengths were approximately 2−3 mm in length (0.5−1.0 nL volume). After the initial packing of the bed, both ends of the capillary were exposed to atmospheric pressure to equilibrate the system. To induce the structures, the magnet was removed to allow the particles to return to their colloidal state. Supraparticle patterns were immediately observed by placing the rare earth magnet 1−2 cm from the microchannel (∼500 G).

Results and Discussion

If one initially flows a dilute colloidal suspension of paramagnetic particles through a cylindrical microchannel where a high magnetic field gradient is present, the particles collect at the area of the steepest gradient.[21] They concentrate on the section of the wall where the strongest attractive force exists and form a close-packed bed. Upon removal of the magnetic field, the particles reform a dispersion because of Brownian motion and electrostatic repulsion. Thus, the colloidal suspension is maintained, even under high volume fraction conditions, and the particles move freely by pressure-induced flow and electrokinetic effects (electroosmosis and electrophoresis). However, upon application of an external magnetic field where there is no appreciable gradient in the axial direction of the microchannel, the particles assume a distinct columnar supraparticle structure (Figures 1 and 2).

(19) Scholten, P. C. *J. Magn. Magn. Mater.* **1983**, *39*, 99−106.
(20) Visscher, P. B.; Gunal, Y. *IEEE Trans. Magn.* **1998**, *34*, 1687−1689.
(21) Joung, J.; Shen, J.; Grodzinski, P. *IEEE Trans. Magn.* **2000**, *36*, 2012−2014.

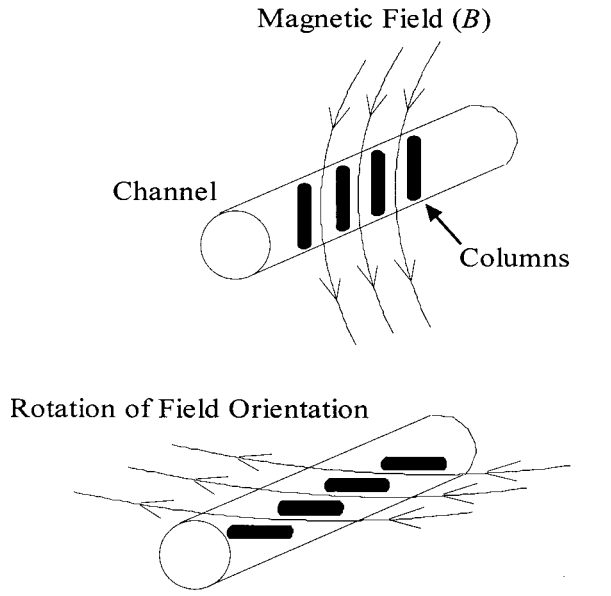

Figure 1. Schematic model indicating magnetic field direction in relation to induced supraparamagnetic structures within a cylindrical channel. The induced structures dynamically align themselves with the applied field without altering their morphology.

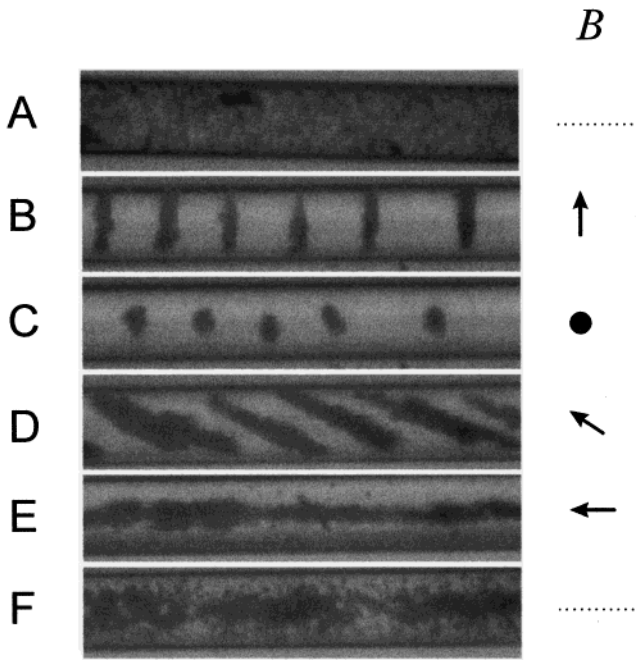

Figure 2. Behavior of paramagnetic particles in cylindrical microchannels (20 μm diameter) as observed by optical microscopy. (A) High volume fraction 1−2 μm diameter aminated paramagnetic particles (Polysciences) in pH 7 phosphate buffer without applied external magnetic field (*B*). (B) Induced columnlike structures that form immediately upon application of external magnetic field where flux is in the plane of page. Upon rotation of applied external magnetic field perpendicular to the page (C), the tops of the columnlike structures are visible. Other patterns result from the field being rotated within the plane of the page but 45° from vertical (D) and aligned with the axis of the channel (E). Upon removal of the external field, the paramagnetic particles immediately resume a colloidal state (F). The elapsed time between image acquisitions was between 1 and 5 s.

According to previous work, the basic structure of the pattern is a function of external field strength and orientation, the container geometry, and the colloid properties.[11,14,15] Although several reports describe similar structures, there are significant differences in the makeup and the dynamics of the structures described here.[11,14,15] For instance, as a consequence of high magnetic flux and parallel field orientation, the structures respond rapidly and reversibly to changes in external field strength and orientation. The responsive structures also move under electrokinetic and pressure pumping while retaining their structural integrity and, because of the surface charge on the solid particles, they return to a colloidal suspension when the magnetic field is removed. This is in contrast to previous experiments where the system properties induced an irreversible phase transition upon structure/pattern formation. The small dimensions and geometry of the channel directly influence the location, spacing, and conformation of the structures. The unique properties in this system have resulted in the discovery of truly dynamic and controllable structures in ultrasmall volumes (nanoliter to picoliter) that can be manipulated through a variety of mechanisms.

Optical microscopy was used to visualize the colloidal suspension and the induced structures, where the data were captured by both video and single-frame imaging. Figure 2A shows a concentrated bed of paramagnetic particles in a dispersed colloidal suspension. This image was acquired without an induced magnetic field, and the bed extended well beyond the 110 μm length shown in this image. It is also important to note that this high volume fraction colloid was free to move by pressure-induced flow or electrokinetic effects and that Brownian motion of individual particles was observed. Upon application of an axially homogeneous magnetic field, where the field was approximately in the plane of the page and vertical, a columnar structure was immediately observed (Figure 2B). Altering the field orientation to be perpendicular to the page immediately resulted in the structures rotating such that the tops of the columns could be viewed (Figure 2C). Note that the structures tend to occupy the central portion of the channel, the caps appear to be cylindrical, and they are somewhat staggered rather than perfectly aligned with the centerline of the tube. Rotation of the field back to the plane of the page but at a 45-degree angle to the original resulted in structures lying parallel but off the vertical axis (Figure 2D). Further rotation to an orientation parallel with the axis of the channel resulted in a ropelike formation aligned down the center of the channel axis (Figure 2E). It is energetically favorable for the paramagnetic particles to form a chain with a length many times greater than the particle diameter.[17] In contrast, the column length in the previous images (Figure 2B−D) was limited by the channel walls, whereas no such limit exists with the field direction along the axis. Once the external magnetic field is removed (Figure 2F), the particles immediately begin diffusing and the structures are relaxed. All of the induced structures (Figure 2B−E) freely move when a pressure gradient or electrokinetic force is applied.

The transition from one pattern to the next because of magnet position and rotation occurs very rapidly, as fast as could be visualized. The retarding forces on the aggregates resulting from viscous drag or interactions with the wall are much weaker than the local and induced magnetic forces. To understand this observation, it is informative to calculate the approximate drag forces versus the influence of reorientation of the external magnetic field. A relative measure of this is obtained by taking the ratio (Ξ) of the force on a paramagnetic particle because of an external field to the drag force[22,23] according

(22) Schramm, L. L.; Clark, B. W. *Colloids Surf.* **1983**, *7*, 135−146.

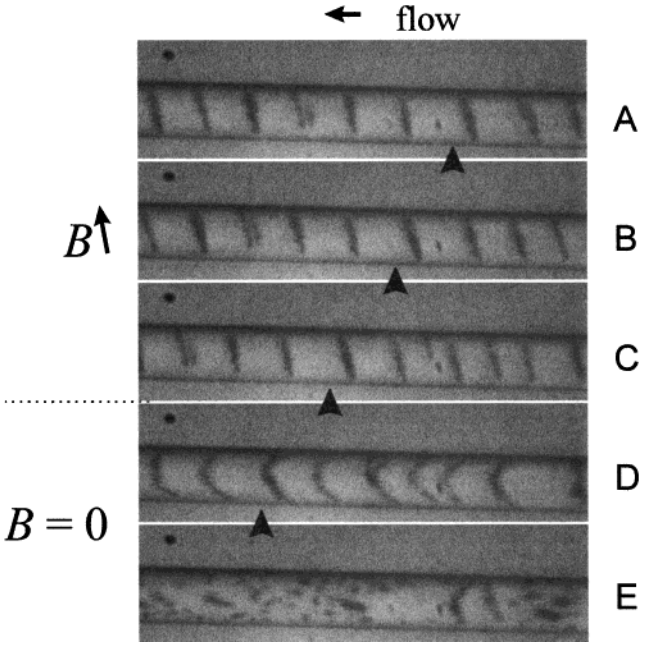

Figure 3. Effects of pressure-induced flow (6.3 pL/s) on supraparticle structures (Polysciences) as observed by optical microscopy. When applied, the external magnetic field is in the plane of the page and approximately vertical. Induced structures are free to move in the presence of flow without distortion (A−C). The arrow emphasizes a particular induced column-like structure being carried along the 20 μm diameter channel. Immediately after the removal of the external magnetic field (D), the shear stresses exerted on structures from the laminar flow profile become apparent as each of the individual particles assumes the local fluid velocity. A short time later, approximately 1 s, the particles have begun to resume a colloidal state (E).

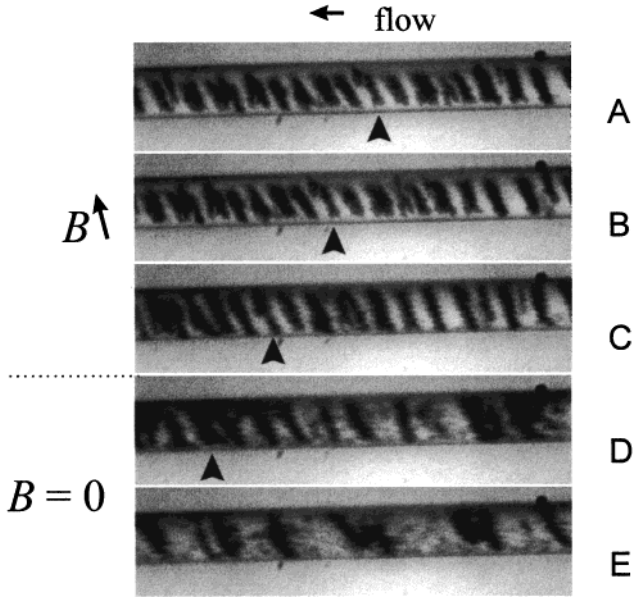

Figure 4. Effects of an applied potential field along the axis of the channel. The potential field generates electrokinetic movement of the induced supraparticle structures (Polysciences) where the observed electrophoretic migration (μ_{obs}) is $(-4.0 \pm 0.2) \times 10^{-4}$ cm^2/Vs ($l = 47.5$ cm, $V_{app} = -374.8$ V; $n = 5$). When applied, the external magnetic field is in the plane of the page and aligned with the arrow next to *B*. Induced structures retain their form in the presence of electrokinetic effects (A−C) where the arrow emphasizes a particular induced structure. Upon removal of the applied magnetic field, the electrokinetic effects still move the individual particles (D and E) as they return to a colloidal state, but no distinct flow pattern is observed because the electrokinetic effects are equivalent across the radius of the 20 μm channel.

to

$$\Xi = (\chi_p - \chi_0) r_p^2 \nabla B^2 / 9\eta\mu_0 U_p \qquad (4)$$

where χ_p is the magnetic susceptibility of the particle, χ_0 is the magnetic susceptibility of the solution, ∇B is the gradient in the magnetic flux density, η is the viscosity of the medium, and U_p is the velocity of the particle. Using a typical neodymium−iron−boron (NdFeB) magnet field strength and assuming a particle velocity of 1 mm/s (a reasonable upper limit in our system), Ξ is greater than 10^4. This indicates that the magnetic force clearly dominates over drag forces in this system. This is significantly different from previous experiments and is a direct result of the very high field intensities achievable with NdFeB magnets (coercivity on the order of 10^6 A/m), as compared to Helmholtz coils or ferromagnets (which are on the order of 10^3 A/m). This 1000-fold higher field intensity provides the rapid response in particle patterning as the field changes, but it does not lock the particles in place. Because the field has no appreciable gradient in the axial dimension, it allows the structures to retain their form while moving laterally under pressure flow or electrokinetic effects (Figures 3 and 4). There is no appreciable force from the induced magnetic field that must be overcome to move the structures in this direction.

For both pressure-induced flow (Figure 3) and electrokinetic effects (electroosmosis and electrophoresis, Figure 4), the individual columns could clearly be visualized while being moved within the small channel. In the case of pressure-induced flow (volume flow 6.3 pL/s, average linear velocity 5 μm/s), laminar flow generates a parabolic profile. It results from the drag induced by the walls and creates a significant change in fluid velocity across the radius of the channel. The highest velocity (twice the average velocity, 10 μm/s), and therefore the highest force on the structures, occurs in the center of the channel, and the lowest velocity is near the wall (in fact, a velocity of zero at the wall). This creates shear stresses across the radius of the channel, the greatest near the walls and the lesser in the center, and therefore across the length of the columns. The structural integrity, induced by local and global magnetic fields, of the columns is sufficient to resist deformation from the flow stresses and any drag effects generated by contact with the walls (Figure 3A−C). The velocity differences can be seen when the external magnetic field is removed; the particles from an individual column immediately assume the local velocity of the flowing stream (Figure 3D,E). The particles in the middle of the channel travel at a higher rate than those at or near the wall in the slower moving lamina. This gives some direct visual evidence of the forces that the structures are able to resist.

Electrokinetic effects use a different mechanism to create movement, and, accordingly, the system behaves differently. Electroosmosis generates a pluglike flow profile, and the velocity is the same at all radii. Electrophoretic forces act directly on the particles themselves because they are positively charged. The columns move at a velocity defined by the additive forces of electrophoresis and electroosmosis, but, again, the structures remain intact and are not deformed by this movement (Figure 4A−C). The observed electrophoretic migration rate (μ_{obs}) of the columnar structures is $(-4.0 \pm 0.2) \times$

(23) Chalmers, J. J.; Zhao, Y.; Nakamura, M.; Melnik, K.; Lasky, L.; Moore, L.; Zborowski, M. *J. Magn. Magn. Mater.* **1999**, *194*, 231−241.

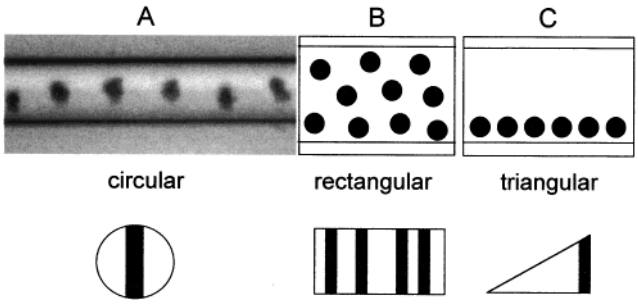

Figure 5. Images and schematics of expected and observed induced structures and resulting patterns for a variety of channel geometries with this system. For all geometries, the external field is perpendicular to the page. For a circular geometry (A), the columnlike structures will form across the central axis to maximize column length. There is no cross-sectional preference in a rectangular geometry (B), and the random but regular spacing generated by column−column repulsion will dominate. In a triangular geometry, the columnlike structures will maximize their length and occupy the tallest portion of the channel (C). The homogeneous length and column−column repulsion should result in very even spacing of the columns in a single plane.

10^{-4} cm^2/Vs. The significant difference in the behavior of this system compared to pressure-induced flow occurs when the external magnetic field is removed (Figure 4D,E), where there is no difference in velocity of the individual particles as a function of radii.

For this system, the fluid mechanics and fast rheologic dynamics associated with rotating the supraparticle structures greater than several rotations per second will need to be explored further. This is noted to emphasize that the flow characteristics in this micron-scale environment with variable structures have yet to be investigated. The externally controlled and independent movement of essentially hard structures in this small system implies that fluid pumps can be devised where the fluid and rheologic studies may suggest specific methodology. This dynamic system promises to be a rich source of investigation in microfluidics.

A general observation from our work concerns container geometry. For cylindrical enclosures, building upon existing columns is preferred, but, once formed, columns may not align themselves perfectly within the center of the tube to achieve maximum volume. Instead, columns are staggered when repulsion between the dipoles from different columns becomes significant. The staggered configuration shows a tradeoff between the energy for column elongation versus intercolumn repulsion. On the basis of this observation and the basic theory of particle interactions, we can predict several new patterns based on altering the microchannel geometry. Figure 5A−C gives several general results for an external field oriented with poles perpendicular to the plane defined by the page. For a rectangular microchannel of similar width, columns will be regularly spaced and distributed evenly within the height or width depending on the orientation of the external magnetic field. Triangular channels will induce other column morphologies based on the tradeoff between extending the column length and repulsion among columns. However, the overall tendency at high concentrations will be toward concentration of columns at the widest part of the channel and equal spacing among columns.

In addition, we would like to add some thoughts on seemingly improbable microchip designs that incorporate the observed phenomenon. The formation mechanism and the dynamic nature of this system lead to a range of issues impacting the design for specific structures or dynamic functions. For instance, the particle diameters which can be used span from the smallest commercially available particles (approximately 20 nm) to a few microns. Width of spacing can be controlled by field strength, particle size, and volume fraction. For example, in general, higher volume fractions lead to smaller spacing. This can be qualitatively observed in images where varying volume fractions are used (Figure 6A−D). The higher volume fraction results in a tighter spacing of the structures (Figure 6A,B). In addition, the particles can be arranged in columns of several particle diameters to single-particle columns (with sufficient field strength) (Figure 6).

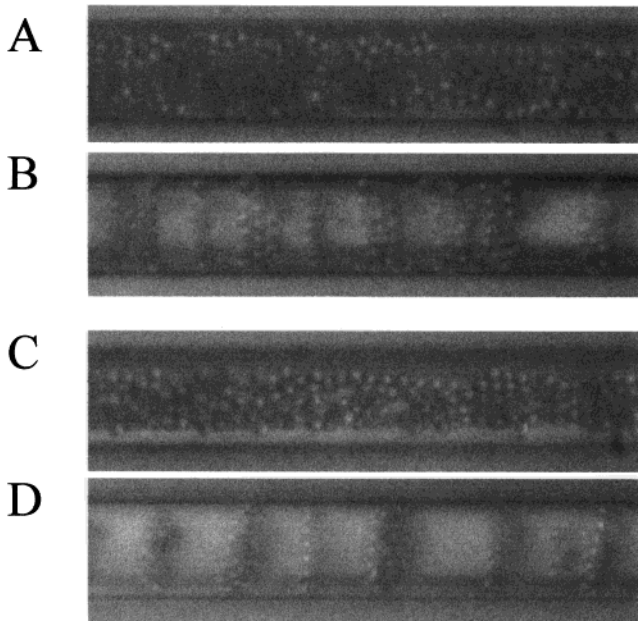

Figure 6. Effects of the paramagnetic particle (Dynal) volume fraction on spacing of aggregate columns in the presence of an external magnetic field perpendicular to the page. A higher volume fraction collected in a packed bed (A). Upon relaxation of the particle bed and reapplication of the magnetic field, columnar structures result (B). A lower volume fraction (C) produces the supraparticle structures that are spaced further apart (D).

Other issues will impact these designs, including particle dispersity, channel size and geometry, volume fraction, and external field strength, orientation, and dynamics. One of the most exciting possibilities is that the spacing and structure of the induced pattern can be made consistent with photon band gap material and therefore a dynamic actuator is possible.[24−28] Also, the line spacing could be dynamically controlled over a considerable range by field strength and/or replacement of the particles by flow to generate ensemble chromatic effects, thus generating a tunable and dynamic grating/interference optical system.[29−31] Varying particle size and aggregate size and spacing can generate other optical effects. These ordered structures which can be molecularly addressed (immunologic interactions, for example) can

(24) Pendry, J. *Science* **1999**, *285*, 1687−1688.
(25) Golosovsky, M.; Saado, Y.; Davidov, D. *Appl. Phys. Lett.* **1999**, *75*, 4168−4170.
(26) Yablonovitch, E. *Phys. Rev. Lett.* **1987**, *58*, 2059.
(27) Yablonovitch, E.; Leung, K. M. *Nature* (*London*) **1998**, *391*, 667.
(28) John, S. *Phys. Rev. Lett.* **1987**, *58*, 2486.
(29) Horng, H.-E.; Hong, C.-Y.; Yeung, W. B.; Yang, H.-C. *Appl. Opt.* **1998**, *37*, 2674−2680.
(30) Davies, P.; Popplewell, J.; Llewellyn, J. P. *IEEE Trans. Magn.* **1988**, *24*, 1662−1664.
(31) Schueller, O. J. A.; Duffy, D. C.; Rogers, J. A.; Brittain, S. T.; Whitesides, G. M. *Sens. Actuators, A* **1999**, *78*, 149−159.

help orient biomolecules for improved resolution for spectroscopic investigations.[32] In addition to spectroscopic bioanalysis, the induced structures can be used to study subcellular biomechanics or to study the effects of intracellular shear forces on cells. Subcellular mixing could also be done through the process of column formation by introducing specific molecular targets for binding the particles prior to structure formation. This could offer the advantage of mixing from within the cell, thus using smaller fluid volumes than currently needed in bulk homogenization techniques. Time can be minimized and energy optimized for homogenization which will improve the yield of active biomolecules.

Another important bioanalysis tool is the movement of externally actuated micron-scale structures to induce convective currents in pico- and femtoliters. This is an area of great interest (microreactions/immunointeractions) and has proven difficult to accomplish by other means.[33,34]

The course of chemical reactions can also be influenced by exploiting the unique properties of the induced suprastructures. The interaction of short-lifetime chemical reaction intermediates (singlet oxygen, for example) can be controlled by manipulating the diffusion path length. Also, the supraparticle structures suggest that they may be able to be combined with a short-chain photoinitiated polymerization to make permanent patterns for nanofabrication for a variety of applications.[16] These include optical elements as described above in a nondynamic version and structural elements which may be used in separation science, filtration, or biological interactions. This patterning, whether permanent or dynamic, can lead to a unique method for creating inexpensive patterned photon masks. By use of these structures in conjunction with more conventional photolithographic techniques, macroscopically controlled microstructures can be created which in turn can be used to pattern the substrates.

Conclusions

Dynamic and reversible supraparticle structures can be formed in microchannels in the presence of a strong external magnetic field. These structures can be rotated freely without deformation during rotation. The supraparticle structures also resist deformation during pressure flow conditions, demonstrating that the attractive forces are much greater than the resulting hydrodynamic forces across the channel diameter. These structures can also be transported through the microchannel by electrokinetic effects. The structures respond rapidly to changes in the external field strength and orientation. Because of the surface charge on the solid particles, they return to a colloidal suspension when the magnetic field is removed. It is expected that the spacing of the structures can be externally controlled and manipulated by altering the volume fraction of the particles, the particle diameters, the magnetic field, and the channel geometry. The unique properties in this system have resulted in the discovery of truly dynamic and controllable structures in ultrasmall volumes that can be manipulated for use in a wide array of potential applications.

Acknowledgment. The authors acknowledge the support from Arizona State University.

LA001655G

(32) Charles, S. W. *J. Magn. Magn. Mater.* **1990**, *85*, 277−284.
(33) Brody, J. P.; Yager, P.; Goldstein, R.; Austin, R. H. *Biophys. J.* **1996**, *71*, 34−3441.
(34) Knight, J. B.; Vishwanath, A.; Brody, J. P.; Austin, R. H. *Phys. Rev. Lett.* **1998**, *80*, 3863−3866.